Vibration and Control of Flexible Rotor Supported by Magnetic Bearings

National Aeronautics and Space Administration
Lewis Research Center
Cleveland Ohio 44135

1. INTRODUCTION

Many papers have been written on magnetic bearings. These papers are divided into two categories: One is the use of magnetic bearings taking the place of contact bearings, and the other is the use of noncontact actuators for active vibration control. These categories are combined in applications. The research on using magnetic bearings in place of contact bearings has been going on for years. As early as 1842 it was known that magnetic bearings should have at least one direction actively controlled [1]. For the last century and a half there has been a great deal of research and development. Magnetic bearings have been used mainly in experiments and in aircraft and missile inertial guidance control. However, these bearings are now coming into use in the industrial world [2] for turbo-molecular pumps [3], machine tool spindles, etc. Although these magnetic bearings are for rigid rotors [4 to 6], they recently have been used with flexible rotors [7 to 9]. In such applications, the magnetic bearings suppress unbalance vibration. Many papers have been published on this subject [10 to 16].

This paper is concerned with active vibration control of flexible rotors supported by magnetic bearings. Using a finite-element method for the mathematical model of a flexible rotor, the author has formulated the eigenvalue problem taking into account the interaction between the mechanical system of a flexible rotor and the electrical system of magnetic bearings and a controller. However, for the sake of simplicity, gyroscopic effects are disregarded herein. It is possible to adapt this formulation to a general flexible rotor - magnetic bearing system. Controllability with and without collocation sensors and actuators located

*National Research Council - NASA Research Associate; on leave from Chiba University, 1-33 Yayoi-cho, Chiba 260 Japan.

at the same distance along the rotor axis is discussed for the higher order flexible modes of the test rig. In conclusion, the author has proposed that it is necessary to add new active control loops for the higher flexible modes even in the case of collocation. It is then possible to stabilize for the case of uncollocation by means of this method.

2. Analysis of Rotor - Magnetic Bearings System for Flexible Rotor [17]

The mathematical model for this flexible rotor is given by using a finite element method:

$$[M]\{\ddot{q}\} + [G]\{\dot{q}\} + [K]\{q\} = \{0\} \tag{1}$$

where [M], [G], and [K] are the mass, gyroscopic, and stiffness matrices, respectively. We assume [G] = 0 for simplicity. Therefore, the X and Y directions are uncoupled. This flexible rotor is now divided into six elements as shown in Fig. 1, and the state values are set as x_i and θ_i at each station. [M], and [K] become 14x14 matrices and {X} vector (instead of {q} vector) of length 14 in the X direction. The flexible rotor is supported by magnetic bearings at stations 2 and 6 and sensors are located at stations 1 and 7. From these results, the formulations in the horizontal direction of the left magnetic bearing shown in Fig. 1 are defined by

$$\left.\begin{aligned} u_{x\ell} &= \frac{4P_\ell}{H_\ell} x_2 - \frac{4P_\ell}{I_\ell} i_{x\ell} \\ E_{1x\ell} - V_{x\ell} &= L \frac{di_{x\ell}}{dt} + Ri_{x\ell} \\ \dot{V}_{x\ell} &= \frac{E_{1x\ell}}{CR_1} - \frac{R_1 + R_2}{CR_1R_2} V_{x\ell} \\ E_{1x\ell} &= - f_{1\ell}x_1 - f_{2\ell}\dot{x}_1 - f_{3\ell}\alpha_\ell \end{aligned}\right\} \tag{2}*$$

where the force $u_{x\ell}$ acts on station 2, and the subscript ℓ means the left magnetic bearing. The steady-state values p_0, h_0, and i_0 are replaced by P_ℓ, H_ℓ, and I_ℓ. The expressions are derived about the right magnetic bearing in the same manner. Combining Eqs. (1) and (2), we can obtain the 34th order state equation as shown in Eq. (3):

$$\frac{d}{dt}\begin{bmatrix} \{X\} \\ \dot{\{X\}} \\ i_{x\ell} \\ \alpha_{x\ell} \\ v_{x\ell} \\ i_{xr} \\ \alpha_{xr} \\ v_{xr} \end{bmatrix} = \begin{bmatrix} \overbrace{[0]}^{28} & [I] & \overbrace{0 \quad 0 \quad 0}^{3} & \overbrace{0 \quad 0 \quad 0}^{3} \\ -[M]^{-1}[K] + \boxed{*1}\frac{4P_\ell}{H_\ell} + \boxed{*6}\frac{4P_r}{H_r} & [0] & -\boxed{*2}\frac{4P_\ell}{I_\ell} \quad 0 \quad 0 & -\boxed{*7}\frac{4P_r}{I_r} \quad 0 \quad 0 \\ -\boxed{*4}\frac{f_{1\ell}}{L} - \boxed{*15}\frac{f'_{1\ell}}{L} & -\boxed{*5}\frac{f_{2\ell}}{L} - \boxed{*16}\frac{f'_{2\ell}}{L} & -\frac{R}{L} \quad -\frac{f_{3\ell}}{L} \quad -\frac{1}{L} & \\ \boxed{*3}1 & [0] & 0 \quad 0 \quad 0 & [0] \\ -\boxed{*11}\frac{f_{1\ell}}{CR_1} - \boxed{*17}\frac{f'_{1\ell}}{CR_1} & -\boxed{*12}\frac{f_{2\ell}}{CR_1} - \boxed{*18}\frac{f'_{2\ell}}{CR_1} & 0 \quad -\frac{f_{3\ell}}{CR_1} \quad -\frac{R_1+R_2}{CR_1R_2} & \\ -\boxed{*9}\frac{f_{1r}}{L} - \boxed{*19}\frac{f'_{1r}}{L} & -\boxed{*10}\frac{f_{2r}}{L} - \boxed{*20}\frac{f'_{2r}}{L} & & -\frac{R}{L} \quad -\frac{f_{3r}}{L} \quad -\frac{1}{L} \\ \boxed{*8}1 & [0] & [0] & 0 \quad 0 \quad 0 \\ -\boxed{*13}\frac{f_{1r}}{CR_1} - \boxed{*21}\frac{f'_{1r}}{CR_1} & -\boxed{*14}\frac{f_{2r}}{CR_1} - \boxed{*22}\frac{f'_{2r}}{CR_1} & & 0 \quad -\frac{f_{3r}}{CR_1} \quad -\frac{R_1+R_2}{CR_1R_2} \end{bmatrix} \begin{bmatrix} \{X\} \\ \dot{\{X\}} \\ i_{x\ell} \\ \alpha_{x\ell} \\ v_{x\ell} \\ i_{xr} \\ \alpha_{xr} \\ v_{xr} \end{bmatrix} \quad (3)$$

(28, 28, 3, 3 / 28, 3, 3)

*1: element (17,3) *6: element (25,11) *11: element (31,1) *16: element (29,19) *21: element (34,9)
*2: element (17,29) *7: element (25,32) *12: element (31,15) *17: element (31,5) *22: element (34,23)
*3: element (30,1) *8: element (33,13) *13: element (34,13) *18: element (31,19)
*4: element (29,1) *9: element (32,13) *14: element (34,27) *19: element (32,9)
*5: element (29,15) *10: element (32,27) *15: element (29,5) *20: element (32,23)

where the subscript r means the right magnetic bearing. In addition, $f'_{1\ell}$, $f'_{2\ell}$, f'_{1r} and f'_{2r} show feedback gains added for active vibration control loops for higher modes. Similarly, we get almost the same equation for the vertical direction. Equation (3) is systematically formulated for a general flexible rotor with magnetic bearings. We can design the control system by solving the eigenvalue problem of Eq. (3) .

3. Experiments

3.1 Test Rig

The laboratory test rotor is shown schematically in Fig. 1. The flexible shaft, which is a 10-mm-diameter drill rod that is 1000 mm long, has five disks with masses as indicated in Fig. 1. The total mass of the flexible rotor is about 3.3 kg. Two of the disks are used for magnetic bearings and two others are used for sensors - i.e, the bearings and sensors are not collocated. The rotor is supported by two magnetic bearings with a

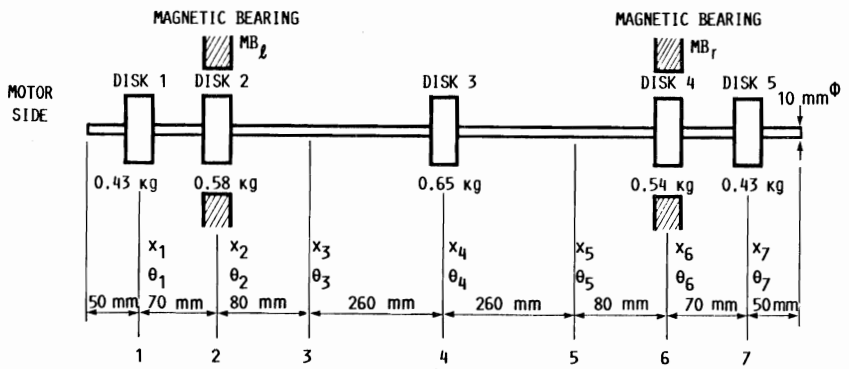

FIG. 1. - SCHEMATIC OF TEST ROTOR.

bearing span length of 680 mm. The shaft is connected to the driving motor by a flexible coupling. This is a radial magnetic bearing system with four degrees of freedom only because the radial directions are non-contacting. The gap between the electromagnets and the disk is about 2.0 mm. The backup bearings protect in an emergency when the amplitudes exceed 1.0 mm. The shaft displacements, which are measured by gap sensors of the eddy current type, are measured as close as possible to the magnetic bearings. These signals are the inputs for the analog controller. The analog controller consists of proportional, differential, and integral circuits, the phase lead circuit, and some filters. The control signals from the analog controllers are supplied to the electromagnets through servoamplifiers.

3.2 Experiments for Flexible Rotor

3.2.1 Critical Speed Map

Figure 2 shows the critical speed map of the rotor model shown in Fig. 1. In the case shown, both stations 2 and 6 are supported by the equivalent spring K. For zero bearing stiffness, there are two rigid modes at 0 Hz, the first bending mode at 20 Hz, the second at 86 Hz, and the third at 130 Hz. The computed free-free data have good agreement with the measured free-free test data shown in Fig. 3. From this, it seems that the mathematical model is correct. The actual critical speeds are estimated as the dot-dash line shown in Fig. 2 using the measured spring constant.

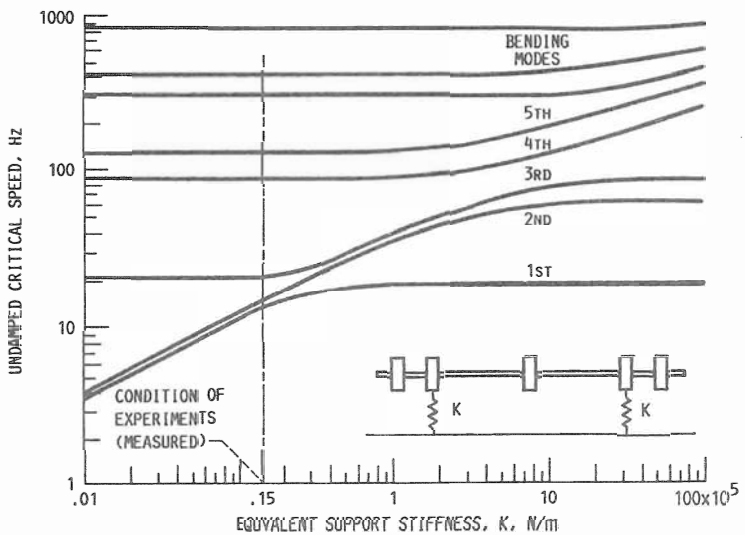

FIG. 2. - CRITICAL SPEED MAP OF THE ROTOR MODEL SHOWN IN FIG. 1.

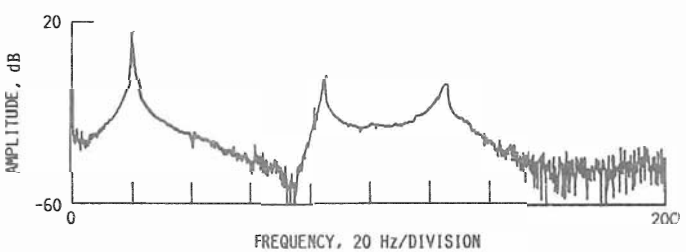

FIG. 3. - MEASURED FREE-FREE TEST DATA.

3.2.2 Frequency Response of Flexible Rotor - Magnetic Bearing System

Figure 4 shows the measured frequency responses of the FFT analyzer based on an impulse response using the same conditions as in Fig. 2. Figure 5 shows measured mode shapes. The first mode at 10.40 Hz is omitted because

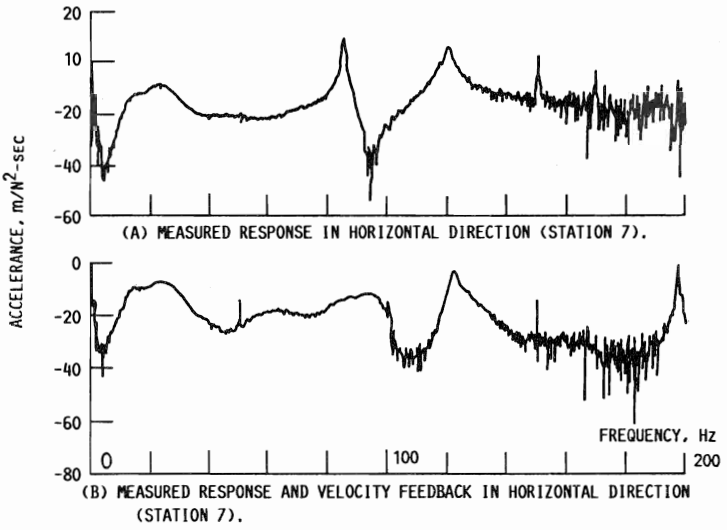

FIG. 4. - MEASURED FREQUENCY, RESPONSE.

it is similar to the second mode. The modal damping ratio at the first mode was $\zeta = 15.04$ percent. The measured critical speeds up to the fifth in Figs. 4 and 5 coincide with the computed critical speeds shown in Fig. 2. The resonance peaks from the first through the third are not clearly recognized because of their high modal damping ratios as shown in Fig. 5.

3.2.3 Eigenvalue Analysis

In this section, we determine the eigenvalues by using Eq. (3). Table I lists the eigenvalues with collocation in the ideal case and Table II shows the eigenvalues without collocation in the case of this experiment. Only complex eigenvalues are listed in the tables and the real roots are omitted. The parameters and feedback gains used for the eigenvalue analysis are the same as those in Section 3.2.2. The results in Table II almost coincide with the results of the critical speeds shown in Figs. 2 and 5. The fourth mode is unstable in Table II. The measured modal damping ratio at 123.13 Hz (as shown in Fig. 5) is too small. Moreover, we cannot pass the fourth critical speed (as shown in Fig. 6) because the amplitudes at locations near the magnetic bearings are growing at speeds greater than 5500 rpm. Therefore, the results of the eigenvalue analysis of Eq. (3) are reasonable. It is possible to design the control system of a flexible rotor - magnetic bearing system by using the eigenvalue analysis of Eq. (3). It is very clear that every mode is stable with collocation. However, the roots of the higher order modes approach the imaginary axis as shown in Table I. Table III shows the improvement of the higher modes

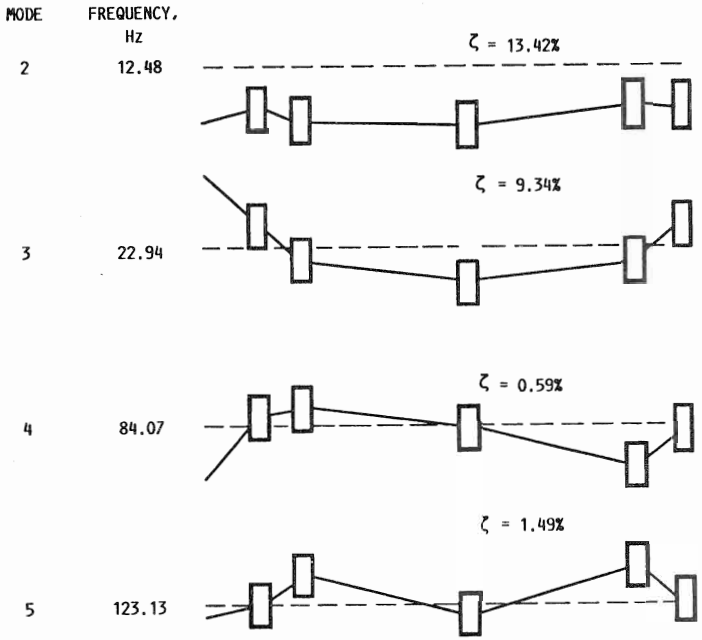

FIG. 5. - MEASURED MODE SHAPES AND MODAL DAMPING RATIOS.

TABLE I. - EIGENVALUES WITH COLLOCATION

Real	Imaginary	Frequency, Hz
-0.22273D-2	0.36128D+5	5750.0
-.22359D-1	.15725D+5	2502.7
-.70242D-1	.12784D+5	2034.6
-.57519D+0	.59381D+4	945.1
-.89774D+1	.29159D+4	464.1
-.22630D+2	.20626D+4	328.3
-.64734D+2	.94692D+3	150.7
-.47460D+2	.66731D+3	106.2
-.82129D+2	.15805D+3	25.2
-.94146D+2	.15287D+3	24.3
-.49705D+1	.12235D+3	19.5

TABLE II. - EIGENVALUES WITHOUT COLLOCATION

Real	Imaginary	Frequency, Hz
0.16181D+2	0.20101D+4	319.9
.74842D+2	.86925D+3	138.3
.71604D+2	.62756D+3	99.9
-.11111D+3	.17393D+3	27.7
-.12722D+3	.15032D+3	23.9
-.65155D+1	.10677D+3	17.0

TABLE III. - EIGENVALUES WITH COLLOCATION IN ADDITION TO VELOCITY FEEDBACK

Real	Imaginary	Frequency, Hz
-0.46911D+3	0.11555D+4	183.9
-.59602D+3	.91103D+3	145.0
-.14625D+3	.36865D+3	58.7
-.28629D+3	.34515D+3	54.9
-.46764D+0	.13729D+3	21.9

with collocations in addition to new velocity feedback loops. The difficulty of passing the higher order critical speeds with collocation is a very important result. Namely, it points out that the usual design method for a rigid rotor has a natural limitation for control of flexible modes. New active control loops are needed for the higher flexible modes even with collocation.

3.2.4 Unbalance Response

Figure 6 shows the unbalance responses for this experiment for the conditions of Section 3.2.2. From these results, both the horizontal and the vertical responses have similar characteristics. There are only low

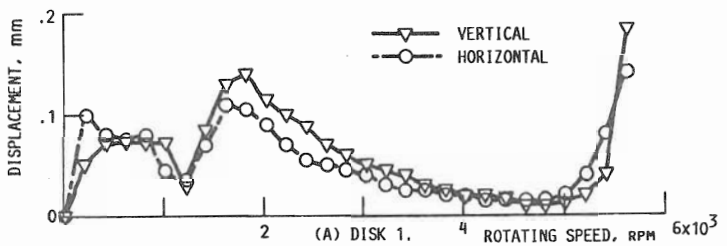

FIG. 6. - UNBALANCE RESPONSES.

amplitude resonances up to 5500 rpm. The rotor should have passed the fourth critical speed by 5500 rpm since the fourth critical speed exists at 84 Hz, 5040 rpm as shown in Fig. 5. Some results indicate that this is caused by gyroscopic effects.

3.2.5 Active Vibration Control

Improving the damping characteristics at the fourth mode is needed in addition to considering the velocity feedbacks $f_{2\ell}'$ and f_{2r}'. Namely, the vibration velocities measured at locations 3 and 5 are used as the control inputs at locations 2 and 6. The results of the eigenvalue analysis for this are shown in Fig. 7. The measured frequency responses by an FFT analyzer are shown in Figs. 4(b). The analysis and experiments show that the characteristics of the fourth mode are improved by active velocity feedback loops. It is possible to pass the fourth critical speed if the dynamic characteristics are as shown in Figs. 4(b). However, it is impossible to pass the fourth critical speed in the actual test rig because of gyroscopic effects. We must design the active vibration control system taking into account the gyroscopic effects of matrix [G] in Eq. (1). The higher order critical speeds can be passed if the flexible rotor - magnetic bearing control system is designed using the stable eigenvalues of Eq. (3) that take into account gyroscopic effects.

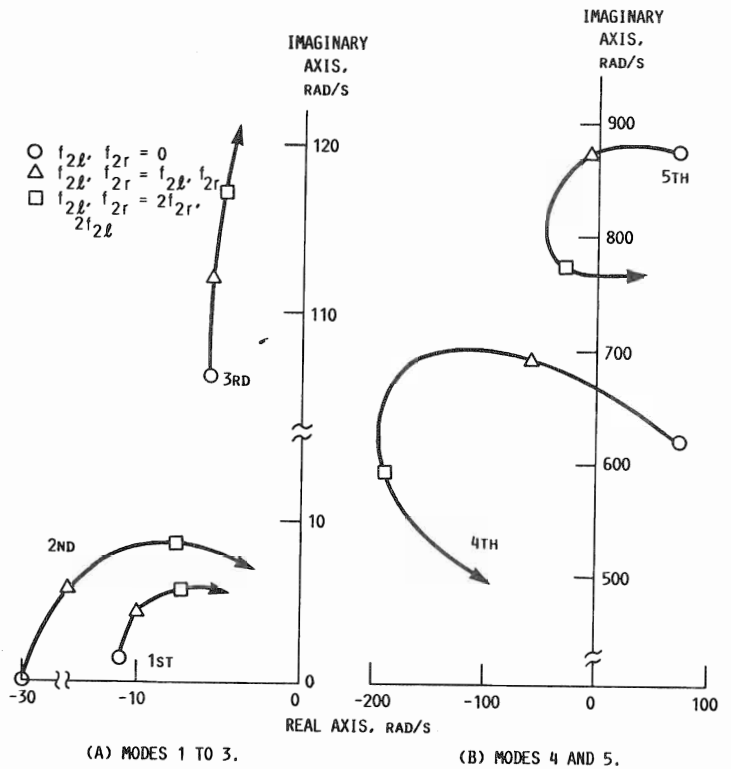

(A) MODES 1 TO 3. (B) MODES 4 AND 5.

FIG. 7. - ROOT LOCI WITHOUT COLLOCATION IN ADDITION TO VELOCITY FEEDBACK.

4. Conclusions

This paper deals with vibration problems and control methods without gyroscopic effects for a flexible rotor supported by radial magnetic bearings with a four-degree-of-freedom system. The conclusions obtained are as follows:

(1) The eigenvalue problem, taking into account the interaction between the mechanical system of a flexible rotor and the electrical system of magnetic bearings and the controller can be formulated as shown herein. The control system of a flexible rotor - magnetic bearing system was designed by an eigenvalue analysis.

(2) If the control system is designed for a rigid rotor, the flexible modes do not become unstable with collocation.

(3) New active control loops must be added for the higher flexible modes even with collocation because the damping characteristics degenerate for the higher order modes. It is possible to stabilize for the case of no collocation by means of this method.

(4) It is not possible to pass the critical speed in the actual test rig even if frequency responses by a FFT analyzer are satisfactory mainly because of gyroscopic effects with rotation.

References

1. Habermann, H.; and Brunet, M.: The Active Magnetic Bearing Enables Optimum Damping of Flexible Rotor. ASME Paper 84-GT-117, 1984.

2. Habermann, H.; and Liard, G.: An Active Magnetic Bearing System. Tribology Int. 13 (1980) 85-89.

3. Foster, E.G.; Kulle, V.; and Peterson, R.A.: The Application of Active Magnetic Bearings to a Natural Gas Pipeline Compressor. ASME Paper 86-GT-61, 1986.

4. Matsumura, F.; Kaobayashi, H.; and Akiyama, Y.: Fundamental Equation for Horizontal Shaft Magnetic Bearing and Its Control System Design. Electr. Eng. Jpn., 101 (3) (1981) 123-130.

5. Matsumura, F.: System and Control, 26 (1982), 209 (in Japanese).

6. Higuchi, T.; and Mizuno, T.: Control System Design for Totally Active DC-Type Magnetic Bearings - Structures of the Optimal Regulator for Systems with Gyroscopic Coupling. Trans. Soc. Instrum. Control Eng., 18 (1982), 507-513 (in Japanese).

7. Allaire, P.E.; Humphris, R.R.; and Kelm, R.D.: Dynamics of a Flexible Rotor in Magnetic Bearings. Rotordynamic Instability Problems in High-Performance Turbomachinery, NASA CP-2443, Washington, D.C.: NASA, 1986, pp. 419-430.

8. Matsushita, O., et al.: Proceedings International Conference on Rotordynamics (1986), 421.

9. Salm, J.R.: Active Electromagnetic Suspension of an Elastic Rotor: Modeling Control and Experimental Results. Rotating Machinery Dynamics. Vol.1, A. Muszynska and J.C. Simonis (eds.) New York: ASME, 1987, pp. 141-149.

10. Schweitzer, G.: Dynamics of Rotors. F.I. Niordson (ed.) New York: Springer-Verlag, 1975, pp. 472.

11. Nikolajsen, J.L.; Holmes, R.; and Gondhalekar, V.: Investigation of an Electromagnetic Damper for Vibration Control of a Transmission Shaft. Proc. Inst. Mech. Eng., 193 (1979), 331-336.

12. Ulbrich, H.; and Anton, E.: Inst. Mech. Eng. Conf. C299/84 (1984) 543.

13. Anton, E.; and Ulbrich, H.: Active Control of Vibrations in the Case of Asymmetrical High-Speed Rotors by Using Magnetic Bearings. J. Vibration Acoustics Stress and Reliability in Design, 107 (1985) 410-415.

14. Salm, J.R.; and Schweitzer, G.: Inst. Mech. Eng. Conf. C277/84 (1984) 553.

15. Okada.,Y., et al.: Trans. Jpn. Soc. Mech. Eng., Vol. 52, No. 467 (1985) 1760 (in Japanese).

16. Matsushita, O., et al.: Trans. Jpn. Soc. Mech. Eng., Vol. 53, No. 496 (1987), 2453 (in Japanese).

17. Nonami, K.: Vibration and Control of Flexible Rotor Supported by Magnetic Bearings. NASA TM-100888, 1988, pp.1-21.

*notes

p_0 : the steady-state attractive force
i_0 : the steady-state current
h_0 : the steady-state gap length
L : the coil inductance
I : the coil current
E_1 : the input voltage to the phase lead circuit
R : the coil resistance
V : the phase lead voltage
f_1, f_2, f_3 : feedback gains

Industrial Applications